

## EVOLUTION OF BORON AND NITROGEN CONTENT DURING ILLITIZATION OF BENTONITES

JAN ŚRODOŃ\*

Institute of Geological Sciences PAN, Senacka 1, 31002 Kraków, Poland

**Abstract**—The incorporation of boron (B) and nitrogen (N) into illite is the key demand-side process responsible for the diagenetic budget of these elements in sedimentary basins, with important implications for pore-water chemistry, natural-gas composition, and borehole geophysics. The purpose of the present study was to take advantage of recent advances in quantitative mineral analysis of sedimentary rocks which have opened new possibilities for investigating this particular process. In order to avoid complications with recycled (detrital) N and B, clays from pyroclastic horizons of sedimentary rocks (bentonites) were used. The B and N contents in illite-smectite were measured in samples from different sedimentary basins, representing a complete range of diagenetic alteration. The bulk-rock chemical measurements, performed on raw rock samples in order to avoid any loss of exchangeable B and N, were referred to the contents of illite-smectite clays and to the content of illite alone, both measured by a combination of XRD and chemistry-based techniques.

Both B and N (as  $\text{NH}_4^+$ ) are present in illite, so their contents in illite-smectite clay increase in a more or less linear manner with progressing illitization. Thus, during diagenesis, the illite-smectite clay is a net consumer of B and N from the pore water. The amount of N in individual illite layers decreases during diagenesis and the amount of B either decreases or remains stable. Bentonitic illite must acquire both B and N from outside of the bentonite bed. In one diagenetic cycle, bentonitic illite fixes up to 800–1000 ppm B and up to >1% N expressed as  $(\text{NH}_4)_2\text{O}$ , corresponding to >20% of the fixed cation sites.

**Key Words**—Ammonium, Bentonite, Boron, Diagenesis, Illite, Smectite.

### INTRODUCTION

Boron (B) and nitrogen (N) are two elements present in clastic sedimentary rocks in small quantities (typically <<1%), which most often are held by the illite+smectite fraction of the rock (see Spivack *et al.*, 1987, for B; Williams and Ferrell, 1991; Lindgreen *et al.*, 2000, for N). The main interest in B behavior in the course of post-sedimentary alterations is generated by hydrochemists, who observe elevated concentrations of B in oilfield brines and other evolved diagenetic waters (*e.g.* Collins, 1975; Zuber and Chowanec, 2009, and literature cited therein), and log analysts, because of the major effect of B on the response of neutron tools (*e.g.* Ellis and Singer, 2007; Zorski *et al.*, in press). Studies of N in clays are most often aimed at using it as an indicator of the reactions generating hydrocarbons, which release N as a by-product (*e.g.* Cooper and Abedin, 1981; Williams *et al.*, 1992; Lindgreen, 1994; Williams *et al.*, 1995; Lindgreen *et al.*, 2000; Środoń *et al.*, 2009a), though the role of mineral nitrogen in the geological nitrogen cycle (Berner, 2006) and the contribution to the nitrogen pool in soils (Holloway and Dahlgren, 1999) have also been stressed.

Since Goldschmidt and Peters (1932), B has been well established as being strongly enriched in shales and

marine sediments with respect to the precursor igneous rocks (from 10 ppm in continental igneous rocks to 100 ppm in shales; Spivack *et al.*, 1987). Two mechanisms of enrichment have been recognized. Adsorption is a reversible, low-temperature process, extracting B from seawater and pore water. Originally B adsorption was investigated as a possible paleosalinity indicator (Frederickson and Reynolds, 1960; Harder, 1970), but later, temperature and pH were documented experimentally as controlling factors (Basset, 1976; Keren and Mezuman, 1981; Palmer *et al.*, 1987). The partition coefficient of exchangeable B increases with pH to ~3.5, but decreases to zero at ~100°C, indicating no B sorption at and above this temperature, and implying mobilization of B adsorbed at lower temperatures (You *et al.*, 1995).

Substitution of B for Si in the tetrahedral sheet of illite is the second enrichment process, dominant in burial diagenetic environments – a result of smectite reaction into illite (Perry, 1972). Such tetrahedral B accounts for 80–90% of B in marine shales, indicating that the observed average B enrichment of shales with respect to igneous rocks is a cumulative product of multiple cycles of weathering and burial (Spivack *et al.*, 1987). Williams *et al.* (2001) pointed to kerogen as a potential source of B during burial diagenesis. According to hydrothermal experiments (You *et al.*, 1995) and field evidence (Spivack *et al.*, 1987), the tetrahedral B is remobilized above 200°C, resulting in a decreased B content of metapelites with increasing metamorphic grade and in redistribution of B among

\* E-mail address of corresponding author:

ndsrodon@cyf-kr.edu.pl

DOI: 10.1346/CCMN.2010.0580602

different mineral phases in other lithologies (Leeman and Sisson, 1996). In particular, Reynolds (1965) observed release of B during metamorphic recrystallization of  $1M_d$  into  $2M_1$  illite in carbonate rocks, resulting in crystallization of magnesian tourmaline (dravite) containing B.

Nitrogen is held by illite in the form of the  $NH_4^+$  cation, substituting for  $K^+$  in illite interlayers. Ammonium is commonly produced by post-sedimentary maturation of the organic matter. Cooper and Abedin (1981), who were first to study the incorporation of  $NH_4^+$  into illite with progressing burial (Gulf Coast), concluded that its content in shales increases systematically with depth, and it does not come from the organic matter present in the rock but it is probably released at greater depth during thermal metamorphism of silicate minerals and organic matter. Cooper and Raabe (1982) made observations consistent with this conclusion when studying N distribution in shales intersected by a basalt dike. Williams and Ferrell (1991) made a similar study of bentonite transected by a dike in the Pierre Shale (Colorado) and concluded that the maximum  $NH_4^+$  fixation takes place at temperatures corresponding to the oil window. This conclusion was supported by Schroeder and McLain (1998), who studied a Gulf Coast oil well. Others, however, have reported illites particularly rich in  $NH_4^+$  from much higher temperatures (hydrothermal alteration zones: Kozáč *et al.*, 1977; Bobos and Ghergari, 1999; anthracite zone: Daniels and Altaner, 1990; Šucha *et al.*, 1994). Recently,  $NH_4^+$  released from the 'temporary storage' in illite and then oxidized by redbeds was indicated as a possible source of N in natural gas of the North German Basin (Mingram *et al.*, 2005).

The present study was initiated in order to understand in more detail the interaction of both B and N with clays during the entire course of post-sedimentary alteration. To avoid complications related to B and  $NH_4^+$  contained in the recycled (detrital) clays, six series of bentonites from different basins were chosen for this study. The clays were analyzed as bulk rocks, without chemical treatment, to ensure that all B and N present in the rock would be measured.

## MATERIALS AND METHODS

In order to make this study representative, six series of bentonite samples, representing different levels of smectite illitization, from different basins around the world, were investigated (Table 1). The Podhale samples are from thin bentonite beds located at the surface of a Tertiary flysch basin, exposing different levels of the diagenetic alteration (Środoń *et al.*, 2006a). The East Slovak Basin (ESB) samples were also from thin bentonites, collected from cores of a Tertiary molasse and characterized mineralogically by Šucha *et al.* (1993). The Welsh Borderlands (WB) are outcrop samples representing thin Silurian bentonite beds alter-

nating with shallow-water limestones (Środoń *et al.*, 1986). The Montana samples came from an outcrop of a thick Upper Cretaceous zoned bentonite (Altaner *et al.*, 1984; Clauer *et al.*, 1997). The Upper Silesia Coal Basin samples were collected in coal mines and represent two thick-zoned bentonite beds of Westphalian (Brzeszcze) and Upper Namurian A (USCB: remaining samples) age (Środoń *et al.*, 2006b).

The untreated rocks were crushed in a hand mortar to pass a 0.4 mm sieve, and were separated with a hand splitter into portions for XRD and chemical analyses. Quantitative XRD mineral compositions were obtained for all 31 samples using ZnO-spiked random preparations and the *QUANTA* computer program (Mystkowski *et al.*, 2002; Omotoso *et al.*, 2006), based on the method of Środoń *et al.* (2001). Compositions were recalculated to 100% (Table 1) and are reported along with the original sum of the *QUANTA* model.

The B and N were measured on splits of untreated bulk rock at the Activation Laboratories, Ltd., [ACTLABS] Canada (B by Prompt Gamma Neutron Activation Analysis (PGNAA, from Thermo Scientific) with a detection limit of 0.5 ppm and N by an elemental analyzer with a detection limit of 0.01% wt.%. The B analyses were checked twice (by ACTLABS, Canada) using two standards, SY-2 and SY-3. For SY-2 the differences between the measurements were 2.5 and 0.5 ppm, and for SY-3, <0.5 ppm. The N analyses were made in duplicate with four samples and all differences were found to be <0.01% absolute. The relative standard deviations calculated for the N analyses of NIST 2684B and NISR 2685B standards were 1.51 and 5.08%, respectively.

$H_2O$  and ethylene glycol monoethyl ether (EGME) sorption and cation exchange capacity (CEC) measurements, following the approach of Środoń *et al.* (2009b) and Środoń (2009) [based on the techniques of Newman (1983) for  $H_2O$ , of Tiller and Smits (1990) for EGME, and of Orsini and Remy (1976) and Bardon *et al.* (1983) for CEC], were performed on the Ca-exchanged bulk-rock samples. A portion of the crushed bulk rock was Ca-saturated by four exchanges with 1 N  $CaCl_2$ , then it was purified by centrifugation followed by dialysis which was monitored by an electrical conductivity meter, and finally freeze dried. All measurements were performed on the same sample split and referred to the same weight at 200°C, which is close to pure dry weight (Środoń and McCarty, 2008).

Another split of the Ca-exchanged bulk-rock sample was used for %  $K_2O$  measurement by a Sherwood Model 420 flame photometer. The results were controlled using NIST 70a and 76a standards (Środoń *et al.*, 2006b), and the measured values differed by no more than 0.01% absolute from the certified values. The %  $K_2O$  measurement was also referred to the weight at 200°C.

For most samples the layer composition of illite-smectite (expressed as %S: percent of smectite layers)

was taken from the original publications (Table 1). This measurement was not available for three of the samples, for which it was carried out in the course of this study. The samples were treated chemically to remove carbonates, organic matter, and Fe oxides (Jackson, 1975). After removing excess electrolytes by centrifuge washing, followed by dialysis, the <0.2 mm fractions were separated and analyzed by X-ray diffraction (XRD) as oriented preparations (10 mg clay/cm<sup>2</sup>) which were air dried and solvated with ethylene glycol. The %S was measured from peak positions (Środoń, 1980, 1984; Środoń *et al.*, 2009b). All available peaks were used and the averaged result was presented.

## RESULTS

Identification based on the XRD patterns of random preparations revealed the following minerals: quartz, smectite or 1*Md* illite-smectite, 2*M<sub>1</sub>* illite+mica, kaolinite, chlorite, K-feldspar, plagioclase (albite or andesine), anatase, pyrite, calcite, ankerite, dolomite, siderite, goethite, hematite, anhydrite, bassanite, and apatite (Figure 1). The rocks investigated represent almost a complete range of interstratification, from a few percent to almost 100%S in illite-smectite (Table 1).

The *QUANTA* results (Table 1) indicate highly variable quantitative mineral compositions among the bentonites studied. Illite-smectite (or smectite) content ranged from 13 to almost 100%, kaolinite from 0 to 52%, chlorite from 0 to 16%, 2*M<sub>1</sub>* mica+illite from 0 to 11%, quartz from almost 0 to >40%, plagioclase from 0 to almost 50%, calcite from 0 to 46%, and K-feldspar and pyrite from 0 to 5%. The remaining components were minor, <3%. The sum of clay minerals ranged from 29 to 99%. The most characteristic compositional differences among the sample sets were: large plagioclase content of the Podhale and East Slovak Basin samples, large chlorite content of the East Slovak Basin samples, large kaolinite content of Brzeszcze samples, and elevated K-feldspar content of the Upper Silesia Coal Basin samples.

## INTERPRETATION

### *Mineral indicators of the degree of post-sedimentary alteration*

The percentage of smectite in illite-smectite (%S) is well established as the best mineral indicator of the degree of diagenesis. No clear correlations between %S and mineral contents were observed in the collected data set.

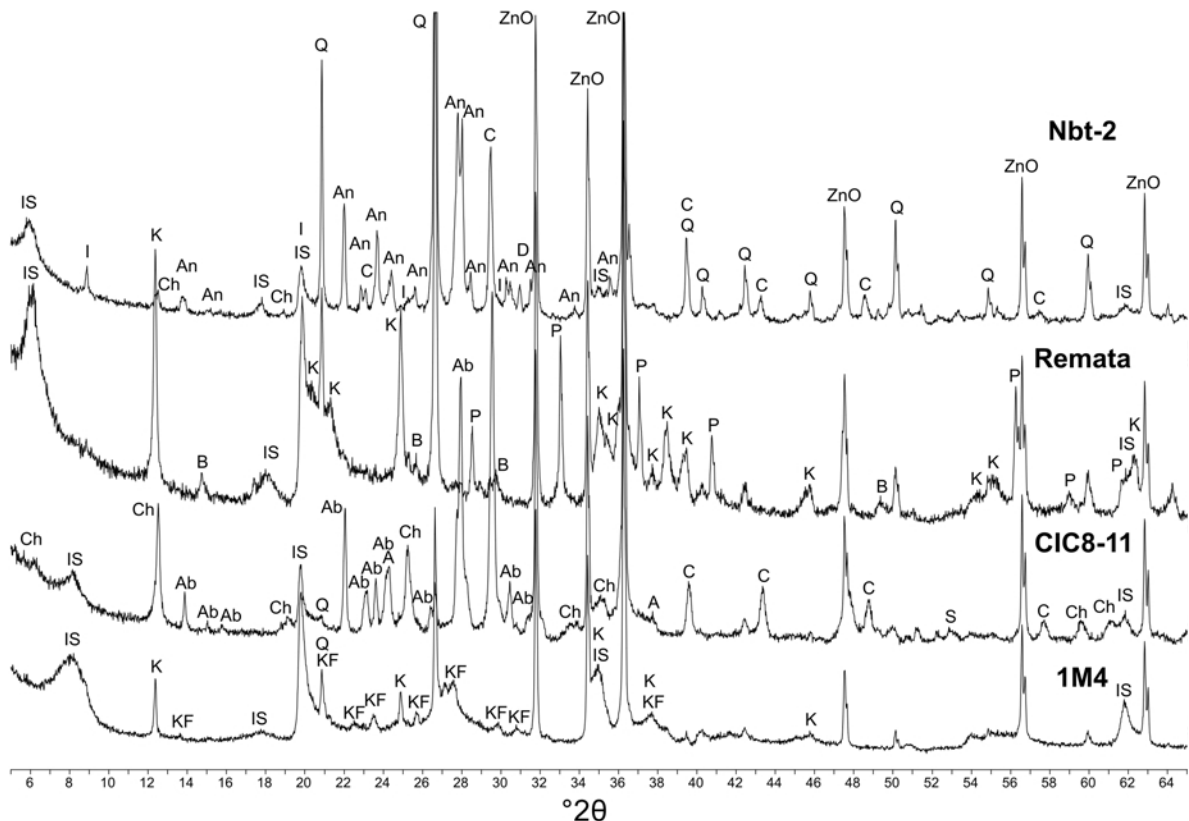


Figure 1. Representative XRD patterns of random preparations of the whole rock with ZnO as internal standard. Q – quartz, IS – smectite or 1*Md* illite-smectite, I – 2*M<sub>1</sub>* illite+mica, K – kaolinite, Ch – chlorite, KF – K-feldspar, Ab – albite, An – andesine, A – anatase, P – pyrite, C – calcite, D – dolomite, S – siderite, B – bassanite.

Table 1. Percent smectite (%S) in illite-smectite, mineral composition of the bulk rocks (raw sum plus wt.% recalculated to 100, \*albite, \*\*andesine, \*\*\* bassanite), and the chemical data (B and N contents, retention of EGME and H<sub>2</sub>O, CEC, and wt.% K<sub>2</sub>O). %S for most of the Podhale samples from Srodoń *et al.* (2006a), for Montana samples from Clauer *et al.* (1997) and S. Altaner (pers. comm.), for WB – Welsh Borderlands, from Srodoń *et al.* (1986), for ESB – East Slovak Basin, from Clauer *et al.* (1997), and unpublished data from that study, for USCB – Upper Silesia Coal Basin, from Srodoń *et al.* (2006b), and for samples MC-7, PROD-1/C, and SA-82-1a measured in this study.

Sample number and region	Locality	%S	Quartz	Kspar	Plagioclase	Anatase	Calcite	Dolomite	Ankerite	Siderite	Pyrite	Goethite	Hematite	Anhydrite	Apatite	Illite 2M <sub>1</sub>	Illite 1M <sub>d</sub> + smectite	Sum 2:1	Kaolinite	Chlorite	Sum Clay	Raw Sum	B (ppm)	N (wt.%)	EGME (mg/g)	H <sub>2</sub> O (mg/g)	CEC (meq/100 g)	K <sub>2</sub> O (wt.%)
<b>Podhale</b>																												
LV-259	Velka Kycera	6	21.4	0	0	0	49.2	0	0	0	0	0	0.2	0	0.7	10.9	12.6	23.5	8.7	0	32.2	105.7	79.1	0.05	14.1	12.0	4.29	2.10
CW-d-1	Male Ciche	26	2.4	0.4	0	1	0	0	0	0	0.3	0	0	0	0	0	73.8	73.8	6.7	0.5	81	97.8	202	0.15	95.4	71.8	42.58	3.01
Kac-1	Kaewin	30	3.2	0	10.2*	0.5	1	0	0.3	0.2	1.3	0	0	0.6	0	3	71.6	74.6	7.5	0.5	82.6	99.4	207	0.19	88.9	67.2	40.34	3.43
Kac-10c	Kaewin	30	5.1	0	10.7*	0.3	2.4	0.4	0	0.3	1.2	0	0	0.2	0.6	4.7	49.3	54	23.5	1	78.5	90.6	163	0.15	71.9	54.2	30.23	2.50
Kac-10d	Kaewin	30	5.6	0.9	32.5*	0.1	5.6	0.1	1.6	0.7	1.6	0.2	0.4	0	0	2.3	30.9	33.2	15.3	2.1	50.6	95.2	103	0.08	44.8	36.0	19.88	1.47
LV-266	Lysa Polana	32	3.8	0.1	20.8*	0.4	1.2	0	0	0.1	0.4	0	0	0.8	0	0	67.5	67.5	2.7	2.1	72.3	93.9	200	0.14	81.4	61.7	35.96	2.87
MC-5	Male Ciche	34	2.9	2.3	13.6*	1.2	0.8	0	0	0.1	0.4	0	0	0	0	0	70.4	70.4	8.2	0	78.6	89.9	194	0.16	90.4	55.7	40.85	2.90
MC-7	Male Ciche	31	3.2	0.5	14.2*	1.5	0.5	0	0	0.8	0.5	0	0	0.3	0	2.7	70.7	73.4	3.8	1.1	78.3	94.9	200	0.17	88.5	64.2	40.68	2.92
BD-0/10a	Bialy Dunajec	34	19.2	0.5	24.8*	0	8.2	0.9	0.3	0	0.6	0	0	0.6	0	0.2	27.2	27.4	2.5	14.9	44.8	107.3	66.6	0.08	40.7	35.3	16.08	1.08
Les-1a	Lesnica	40	4.3	0	16**	0.2	0	0	0	1.6	0.1	1.4	0	0	0	1.8	51.8	53.6	20.3	2.5	76.4	146.4	77.2	0.12	82.4	61.4	26.92	1.69
Rat-1	Ratulów	66	11.5	0	16.3**	0.3	4.2	0	0.7	0.2	0.4	0	0.1	0.2	0.7	3.1	59	62.1	3.4	0	65.5	97.8	120	0.07	111.6	88.9	55.00	2.24
Nbt-2	Nowe Bystre	78	31.9	0.5	26**	0	9.4	1	0.9	1.1	0	0	0	0	0	5.1	18.5	23.6	3.7	2	29.3	94.7	51.9	0.06	43.4	39.7	20.09	1.32
LV256/B	Bystre	95	4.6	1.3	49.9**	0.3	1.9	0.1	0.1	1.1	0	1.1	0	0	0	0.5	39.1	39.6	0	0	39.6	93.1	24.7	0.1	106.7	79.4	46.01	1.01
Remata	Remata	90	11.4	0	0	0.7	0	0	0	0.1	4.8	2.4	1.1	0.2***	0.7	2.5	33.1	35.6	42.4	0.7	78.7	138.6	43.1	0.06	107.3	68.1	35.95	0.58
PROD-1/B	Prosiecka valley	80	4.6	0	31.9**	0.2	3.4	0	0.1	0.3	5.5	0.2	0.2	0.1	0	0	45.7	45.7	7.8	0	53.5	94.1	39.7	0.09	79.0	70.4	42.77	0.72
PROD-1/C	Prosiecka valley	75	9.1	1.4	24.4**	0	0.7	0	0	0.6	0	2.2	0.1	0	1.1	3.4	48.6	52	7.1	1.2	60.3	86.2	62.7	0.09	101.7	82.4	50.84	1.42
HU-4/1	Huty	41	10	0.2	27.8*	0.1	0.3	0	0	0.6	0.5	0.1	0	0.1	0	2.5	23.3	25.8	34.6	0	60.4	98.2	60.7	0.1	47.0	42.3	20.24	1.12
HU-4/2	Huty	64	21.2	0	26.3*	0.3	0	0	0	1.6	0	0	0	0.1	0	4.5	25.5	30	17.6	2.9	50.5	95.9	66.4	0.1	50.5	43.7	18.85	1.38
LV-98	Bajenovec	44	2	0	29.4*	0	0.3	0	0	0	0	0	0	0.8	0	0	47.9	47.9	19.5	0	67.4	102.4	137	0.07	91.4	67.0	37.84	1.71
<b>Montana</b>																												
SA-11a	Sun River Canyon	32	14.4	0	3**	0	1	0	0	0	0.3	0	0	0	0	0	77.8	77.8	3.1	0.5	81.4	99.9	106	0.15	92.8	68.3	37.11	4.14
SA-82-2i	Sun River Canyon	60	36.8	0	4.7**	0	1.5	0	0	0.3	0	0	0	0	0.2	0	51.4	51.4	2.5	2.5	56.4	99.3	47.6	0.1	76.2	63.9	34.91	2.01
SA-82-1a	Sun River Canyon	36	21	0	2.4*	0	1.7	0	0	0.1	0	0	0	0	0	1.4	69.8	71.2	3.4	0.1	74.7	103	97.6	0.16	93.5	72.0	39.18	3.72
SA-82-2b	Sun River Canyon	33	21.6	0.9	3.1*	0	0.9	0.1	0	0	0.3	0	0.1	0.5	0.4	0	69.9	69.9	2.1	0.1	72.1	96.7	91.7	0.15	84.4	68.9	35.32	3.72



### Mineral indicators of the degree of epiclastic contamination

Di octahedral mica (illite)  $2M_1$  is a mineral component that is absent from the pyroclastic materials, and as such may serve as an indicator of epiclastic contamination of bentonites. In most samples,  $2M_1$  was absent or barely detectable, but occasionally elevated contents (up to 5%; in one sample 11%) were observed. The  $\%2M_1$  was not correlated with the content of any other mineral.

### Evaluation of authigenic illite and smectite contents of the rocks

Measurements of authigenic illite and smectite are crucial for tracing the diagenetic evolution of the B and N contents based on bulk-rock analyses, *i.e.* for the approach used in this study. Recent advances of quantitative XRD analysis allow for the accurate evaluation of the sum of all di octahedral 2:1 clays (hereafter  $\%2:1$ ), and also for differentiating  $1Md + \text{turbostratic}$  (illite + smectite; hereafter  $\%I+S$ ) and  $2M_1$  polytype (illite + mica; hereafter  $\%2M_1$ ) (*e.g.* Środoń *et al.*, 2001; Omotoso *et al.*, 2006). Separate evaluation of illite and smectite contents of the rock with comparable accuracy is not possible by XRD quantitative analysis. Chemistry-based techniques of such measurement were proposed recently (Środoń *et al.*, 2009b; Środoń, 2009) and they have been applied in this study, along with a mixed technique, using a calibration of the XRD measurement of  $\%S$ .

The calculation of illite content (defined as the sum of all non-expandable interlayers of authigenic 2:1 clays) was based on the finding of Środoń *et al.* (2009b) that the charge of illite layers is stable and equals  $0.95/O_{10}(OH)_2$ . If the fixed interlayer cation is only  $K^+$ , then this charge corresponds to  $\sim 11\%$   $K_2O$  in the di octahedral aluminous illite. Thus, the illite content of the rock ( $f_i$ ) can be calculated by dividing the  $K_2O$  content of the rock assigned to the authigenic 2:1 clay ( $\%I+S$ ) by 11%.

Precise calculation should account for  $NH_4^+$  substitution in illite. Bentonites are rocks essentially devoid of organic matter. Potassium feldspar, another possible carrier of N, is present in trace amounts in most samples, and in the Carboniferous samples, where it is more abundant (Table 1), it was identified as volcanogenic, not authigenic (Środoń, 1976). Based on these data, assigning all N to the authigenic illite-smectite was considered to be a justifiable approximation. The N measured in the rocks was recalculated into  $(NH_4)_2O$ , then into an equivalent amount of  $K_2O$ , and added to the measured  $K_2O$  giving  $K_2O_{\text{corr}}$ .  $K_2O$  in K-feldspar and in  $2M_1$  mica was then calculated from their XRD contents, assuming typical values of 15%  $K_2O$  in K-feldspar ( $\sim 10\%$  of Na for K substitution) and 11%  $K_2O$  in illite. Subtracting these values from  $K_2O_{\text{corr}}$  produced a  $K_2O$  content of the rock representing the authigenic clay,

which also accounted for the  $(NH_4)_2O$  contribution (Table 2).

An alternative technique for calculating  $f_i$  is based on the experimental relationship between  $\%K_2O$  (including recalculated  $(NH_4)_2O$ ) in illite-smectite and  $\%S$ , established from the data of Środoń *et al.* (2009b) obtained for pure illite-smectites:

$$\%K_2O = 0.0006*\%S^2 - 0.1628*\%S + 10.855 \quad r^2 = 0.99 \quad (1)$$

Multiplying this value by the fraction of authigenic 2:1 clay in the rock ( $\%I+S = \%2:1 - \%2M_1$ ) produces  $\%K_2O$  (including  $(NH_4)_2O$  recalculated to  $K_2O$ ) in the rock representing the authigenic clay. Such calculation is possible only in bentonites, where all of the 2:1 fraction, except the  $2M_1$  illite, is a single authigenic, homogenous illite-smectite.

The two calculations of  $f_i$  were compared (Figure 2) and gave a linear relationship ( $r^2 = 0.93$ ) which extrapolated to zero, although the values based on  $\%S$  were systematically greater. Some discrepancies were expected because the two calculations were based on four XRD quantitative measurements ( $\%S$ ,  $\%K_{\text{spar}}$ ,  $\%2:1$ ,  $\%2M_1$ ), which are not as accurate as the chemical measurements.

The smectite (defined as the sum of all expandable interlayers including edges of 2:1 clays; Środoń *et al.*, 2009a, 2009b) content of the rock ( $f_s$ ) can be calculated analogously to  $f_i$ , as the ratio of the total specific surface area (TSSA) of the rock to the TSSA of pure smectite, if other components with large TSSA values are negligible. Środoń (2009) demonstrated that the calculation of the rock TSSA can be based on CEC and EGME retention, if their relationship is linear and if the data extrapolate to zero. Such a relationship for the bentonite samples under study (Figure 3) was close enough to the data of Środoń (2009) to assume that the approach used in this paper can be applied.  $H_2O$  sorption data (Table 2) were not used for the  $f_s$  calculation because they confirm the excess

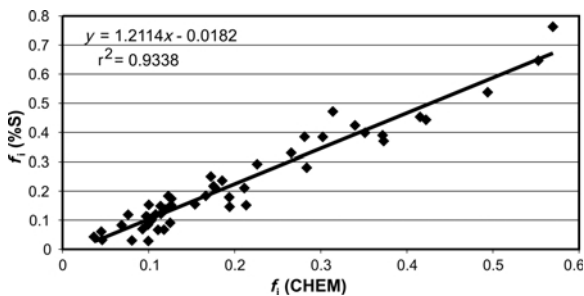


Figure 2. Comparison of two independent calculations of the illite fraction of the rock ( $f_i$ ) from the K and  $NH_4$  contents in the rock assigned to illite:  $f_i$  (CHEM) – measured after correction for K-feldspar, and  $f_i$  (%S) – calculated from illite-smectite layer composition (equation 1) and illite+smectite content (XRD data); details in the text.

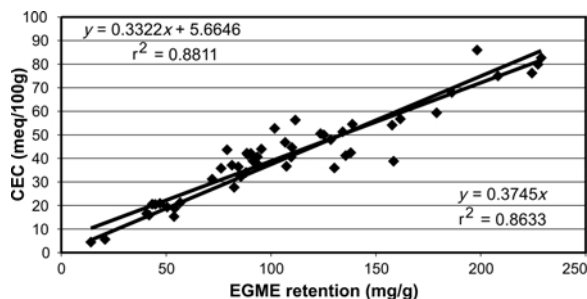


Figure 3. The plot of EGME retention vs. CEC, used to infer the values of smectitic layer charge and EGME coverage, needed for the calculation of the smectite fraction of the rock ( $f_s$ ).

water at low CEC values which was detected in the 2009 study. The calculations of  $f_s$  from the CEC and EGME data (Table 2) were based on equations 1 and 2 of Środoń (2009), *i.e.*

$$\text{TSSA(EGME)} = \frac{\text{EGME}_{\text{retention}}}{\text{EGME}_{\text{coverage}}} \quad \text{and}$$

$$\text{TSSA(CEC)} = \frac{\text{CEC} \times b_0^2 \times \text{EGME} \times 3.477}{Q_s}$$

where the mean smectite TSSA is  $757 \text{ m}^2/\text{g}$ , the mean  $b_0$  for aluminous dioctahedral 2:1 clays is  $0.9 \text{ nm}$ , smectitic charge ( $Q_s$ ) is  $0.41/\text{O}_{10}(\text{OH})_2$ , and the EGME coverage is  $0.41 \text{ mg/m}^2$ :

$$f_s = 0.0091 * \text{CEC} \quad (2)$$

$$f_s = \text{EGME retention}/310 \quad (3)$$

The correlation of the two values (Figure 4) was linear and quite strong, but the EGME-based values were slightly smaller than the CEC-based values.

The  $f_i$  and  $f_s$  values were averaged and their sum plotted vs. % authigenic illite + smectite measured by XRD (Figure 5). The high linear correlation extrapolating to zero demonstrated that the XRD and chemistry-based measurements were internally consistent. A justified assumption is, therefore, that the estimates of  $f_i$  and  $f_s$  are accurate and precise enough to be used for analyzing the evolution of the B and N contents in the

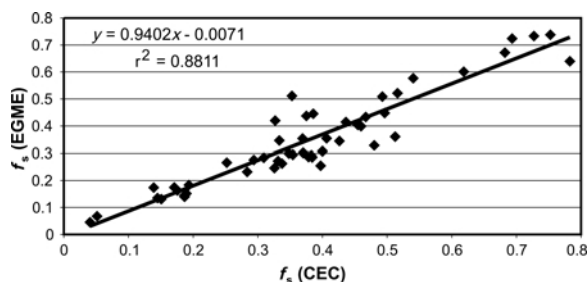


Figure 4. Comparison of two independent calculations of the smectite fraction of the rock ( $f_s$ ): from measured CEC using equation 2 and from measured EGME retention using equation 3; details in the text.

course of illitization. The averaged values of  $f_i$ ,  $f_s$ , and  $f_{(i+s)}$  (Table 2) were, therefore, used in further calculations. The individual values were also tried, but the differences between them were too small to affect the final conclusions concerning B and  $\text{NH}_4^+$  behavior.

#### Evolution of the B and N contents during diagenesis

The B and N contents of the rock were plotted against the content of authigenic 2:1 clay (%I+S), separately for the different series of bentonites (Figure 6a,b). No general relationship was detected. For three of the series, a tendency to positive correlation was observed for both elements; for the other three, such tendencies were absent. Plotting the same values against the illite content in the rock yielded a generally positive correlation (Figure 7a,b). The different bentonite series formed more or less coherent linear plots with different slopes, all extrapolating close to zero. These plots demonstrate that most if not all of the B and N present in the rock are contained in the authigenic illite. If significant amounts of B and N were contained in the rock components other than illite (*e.g.* in smectite), then the plots in Figure 7 would extrapolate to positive values for 0% illite. This assertion was confirmed by plotting the B and N contents of the authigenic 2:1 clay (recalculated from the bulk-rock contents) against the degree of illitization expressed by %S (Figure 8a,b), which gave clear negative correlations for all sets. During illitization, the contents of both elements in the authigenic 2:1 clays increased several fold.

The B and N contents of the rock were also recalculated into the contents of these elements in the authigenic illite (B in ppm and N as % of fixed cation sites occupied by  $\text{NH}_4^+$ ) and also these values were plotted vs. %S (Figure 9a,b). The surprising result was that the B contents in the illite layers were either stable or decreased during the course of illitization. The N content decreased in all investigated series.

The range of amounts of illite was quite large, from <200 to >1000 ppm for B and from 5 to >35% of fixed cation sites for  $\text{NH}_4^+$  (the values for extremely large %S are less reliable because of the large relative error of the % illite layers measurement). For all series, except the

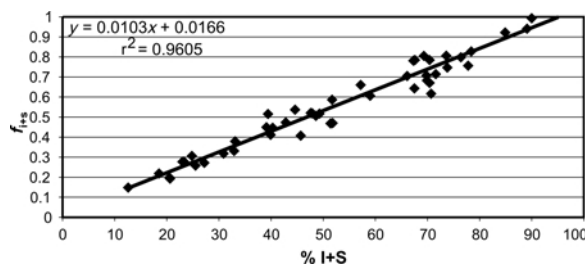


Figure 5. Comparison of two independent calculations of the illite+smectite content of the rock: from chemistry ( $f_{i+s}$ ) and from XRD (%I+S); details in the text.

Table 2. Calculation of %N as  $\%(\text{NH}_4)_2\text{O}$  and the equivalent  $\%\text{K}_2\text{O}$ ,  $\%\text{K}_2\text{O}$  corrected for ammonium,  $\%\text{K}_2\text{O}$  in illite and the fraction of illite in the rock ( $f_i$ ) by two techniques, corrected CEC, and fraction of smectite in the rock ( $f_s$ ) by two techniques, and B and  $\text{NH}_4^+$  content of illite-smectite and illite (see text for details).

Sample number and region	% $(\text{NH}_4)_2\text{O}$	$\%\text{K}_2\text{O}$ equiv. corr.	$\%\text{K}_2\text{O}$ illite from CHEM	$\%\text{K}_2\text{O}$ illite from %S	CEC corr.	$f_i$ (CHEM)	$f_i$ (%S)	$f_i$ mean	$f_s$ (CEC)	$f_s$ (EGME)	$f_s$ mean	$f_{(i+s)}$ mean	%I+S (%)	B in IS from %I+S (ppm)	B in IS from $f_{(i+s)}$ (ppm)	mean B in IS (ppm)	B in illite (ppm)	% $\text{NH}_4$ in IS from %I+S	% $\text{NH}_4$ in IS from $f_{(i+s)}$	mean % $\text{NH}_4$ in IS	%subst. $\text{NH}_4$ for K in I		
<b>Podhale</b>																							
LV-259	0.09	0.17	2.27	1.07	1.25	4.45	0.10	0.11	0.11	0.04	0.05	0.04	0.15	13	627.8	533.5	580.6	751.2	0.74	0.63	0.68	14.51	
CW-d-1	0.28	0.50	3.51	3.45	5.19	43.95	0.31	0.47	0.39	0.40	0.31	0.35	0.75	74	273.7	270.6	272.1	514.3	0.38	0.37	0.38	11.67	
Kac-1	0.35	0.64	4.07	3.74	4.66	41.60	0.34	0.42	0.38	0.38	0.29	0.33	0.71	72	289.1	289.7	289.4	542.1	0.49	0.49	0.49	15.20	
Kac-10c	0.28	0.50	3.00	2.49	3.21	31.18	0.29	0.29	0.26	0.28	0.23	0.26	0.52	49	50	330.6	315.4	323.0	629.4	0.57	0.54	0.55	17.70
Kac-10d	0.15	0.27	1.74	1.35	2.01	20.50	0.12	0.18	0.15	0.19	0.14	0.17	0.32	31	31	333.3	323.5	328.4	673.8	0.48	0.47	0.47	15.99
LV-266	0.26	0.47	3.34	3.33	4.23	37.07	0.30	0.38	0.34	0.34	0.26	0.30	0.64	68	66	296.3	310.9	303.6	582.7	0.39	0.40	0.40	12.46
MC-5	0.30	0.54	3.44	3.09	4.23	42.10	0.28	0.38	0.33	0.38	0.29	0.34	0.67	70	69	275.6	289.4	282.5	582.6	0.42	0.44	0.43	14.68
MC-7	0.32	0.57	3.49	3.12	4.51	42.22	0.28	0.41	0.35	0.38	0.29	0.33	0.68	71	69	282.9	293.9	288.4	576.4	0.45	0.46	0.46	14.97
BD-0/10a	0.15	0.27	1.35	1.25	1.64	16.57	0.11	0.15	0.13	0.15	0.13	0.14	0.27	27	27	244.9	244.6	244.7	507.4	0.55	0.55	0.55	18.62
Les-1a	0.22	0.40	2.09	1.90	2.75	27.71	0.17	0.25	0.21	0.25	0.27	0.26	0.47	52	49	149.0	164.3	156.6	365.9	0.43	0.47	0.45	17.38
Rat-1	0.13	0.24	2.48	2.13	1.61	56.31	0.19	0.15	0.17	0.51	0.36	0.44	0.61	59	60	203.4	197.9	200.7	705.6	0.22	0.21	0.22	12.58
Nbt-2	0.11	0.20	1.52	0.89	0.33	20.52	0.08	0.03	0.06	0.19	0.14	0.16	0.22	19	20	280.5	237.2	258.9	935.9	0.60	0.51	0.56	33.06
LV256/B	0.19	0.34	1.35	1.10	0.31	46.82	0.10	0.03	0.06	0.43	0.34	0.39	0.45	39	45	63.2	55.0	55.0	385.3	0.48	0.41	0.41	47.66
Remata	0.11	0.20	0.78	0.51	0.35	36.62	0.05	0.03	0.04	0.33	0.35	0.34	0.38	33	35	130.2	113.8	122.0	1104.4	0.34	0.29	0.32	46.98
PROD-1/B	0.17	0.30	1.02	1.02	0.76	43.66	0.09	0.07	0.08	0.40	0.25	0.33	0.41	46	43	86.9	97.5	92.2	489.0	0.37	0.41	0.39	33.87
PROD-1/C	0.17	0.30	1.72	1.14	0.98	52.76	0.10	0.09	0.10	0.48	0.33	0.40	0.50	49	49	129.0	126.2	127.6	650.6	0.34	0.34	0.34	28.54
HU-4/1	0.19	0.34	1.46	1.15	1.21	20.83	0.10	0.11	0.11	0.19	0.15	0.17	0.28	23	26	260.5	218.5	239.5	565.8	0.80	0.67	0.73	28.48
HU-4/2	0.19	0.34	1.72	1.22	0.74	19.31	0.11	0.07	0.09	0.18	0.16	0.17	0.26	26	26	260.4	257.0	258.7	745.7	0.73	0.72	0.72	34.32
LV-98	0.13	0.24	1.95	1.95	2.32	38.91	0.18	0.21	0.19	0.35	0.29	0.32	0.52	48	50	286.0	264.2	275.1	705.8	0.27	0.25	0.26	11.02
<b>Montana</b>																							
SA-11a	0.28	0.50	4.64	4.64	4.87	38.26	0.42	0.44	0.43	0.35	0.30	0.32	0.76	78	77	136.2	140.2	138.2	245.1	0.36	0.37	0.36	10.60
SA-82-2i	0.19	0.34	2.35	2.35	1.67	35.78	0.21	0.15	0.18	0.33	0.25	0.29	0.47	51	49	92.6	101.7	97.1	260.8	0.36	0.40	0.38	16.74
SA-82-1a	0.30	0.54	4.26	4.10	4.03	40.66	0.37	0.37	0.37	0.37	0.30	0.34	0.70	70	70	139.8	138.6	139.2	264.0	0.43	0.42	0.42	13.23
SA-82-2b	0.28	0.50	4.22	4.09	4.29	36.40	0.37	0.39	0.38	0.33	0.27	0.30	0.68	70	69	131.2	134.3	132.8	240.8	0.40	0.41	0.40	12.04
<b>WB</b>																							
MI						38.77				0.35	0.51		98										
M2	0.17	0.30	5.53	5.43	5.91	47.95	0.49	0.54	0.52	0.44	0.41	0.43	0.94	89	92	160.5	151.9	156.2	277.2	0.19	0.18	0.18	5.33
M3	0.15	0.27	2.73	2.32	2.31	86.00	0.21	0.21	0.21	0.78	0.64	0.71	0.92	85	89	46.9	43.2	45.0	188.9	0.18	0.16	0.17	11.60
M5	0.20	0.37	6.11	6.08	7.11	42.38	0.55	0.65	0.60	0.39	0.45	0.42	1.01	99	100	181.3	177.4	179.3	300.2	0.21	0.20	0.20	5.61
M7	0.24	0.44	6.27	6.27	8.39	35.92	0.57	0.76	0.67	0.33	0.42	0.37	1.04	95	99	183.4	167.4	175.4	261.2	0.25	0.23	0.24	5.96
M9	0.20	0.37	4.81	4.57	4.98	59.37	0.42	0.45	0.43	0.54	0.58	0.56	0.99	90	95	188.9	171.2	180.1	391.7	0.23	0.21	0.22	7.74
<b>ESB</b>																							
TRH 1/37	0.11	0.20	1.51	1.39	1.66	5.65	0.13	0.15	0.14	0.05	0.07	0.06	0.20	21	20	480.5	497.0	488.8	709.8	0.54	0.56	0.55	13.21
CIC 8/11	0.20	0.37	1.83	1.83	2.02	15.29	0.17	0.18	0.17	0.14	0.17	0.16	0.33	33	33	243.8	242.1	242.9	458.5	0.62	0.62	0.62	19.21
CIC 1/20	0.11	0.20	1.39	1.39	1.91	33.99	0.13	0.17	0.15	0.31	0.28	0.30	0.45	40	42	58.8	53.0	55.9	157.8	0.28	0.25	0.26	12.21
CIC 1/18	0.07	0.13	1.12	1.10	1.68	32.29	0.10	0.15	0.13	0.29	0.28	0.28	0.41	40	41	86.5	83.8	85.1	272.6	0.19	0.18	0.18	9.66
PRT 10/10	0.07	0.13	0.49	0.49	0.67	15.92	0.04	0.06	0.05	0.14	0.14	0.14	0.19	21	20	164.6	175.7	170.2	641.1	0.36	0.39	0.37	23.11



USCB	0.15	0.27	3.91	3.86	4.38	41.22	0.35	0.40	0.37	0.38	0.44	0.41	0.78	67	73	194.7	167.7	181.2	349.5	0.22	0.19	0.21	6.52
Ch4	0.09	0.17	4.00	2.92	3.62	54.14	0.27	0.33	0.30	0.49	0.51	0.50	0.80	76	78	217.3	207.9	212.6	557.9	0.12	0.12	0.12	5.13
IM4	0.11	0.20	2.79	2.13	1.97	56.73	0.19	0.18	0.19	0.52	0.52	0.52	0.71	66	68	138.9	130.2	134.5	492.7	0.17	0.16	0.16	9.84
1Cz2	0.07	0.13	2.71	2.04	2.59	51.31	0.19	0.24	0.21	0.47	0.43	0.45	0.66	57	62	128.8	111.6	120.2	350.2	0.13	0.11	0.12	5.81
2M0	0.09	0.17	2.63	1.93	2.39	67.98	0.18	0.22	0.20	0.62	0.60	0.61	0.81	74	77	118.2	107.9	113.1	443.2	0.13	0.12	0.12	7.78
2M3	0.06	0.10	1.73	1.31	1.50	74.95	0.12	0.14	0.13	0.68	0.67	0.68	0.80	69	75	101.9	87.7	94.8	551.3	0.08	0.07	0.07	7.16
1Cz3	0.04	0.07	1.60	0.84	1.31	79.91	0.08	0.12	0.10	0.73	0.73	0.73	0.83	78	81	109.7	103.9	106.8	881.1	0.05	0.04	0.05	6.26
2M6	0.06	0.10	1.22	0.76	0.91	76.19	0.07	0.08	0.08	0.69	0.72	0.71	0.78	68	73	71.4	61.6	66.5	636.4	0.08	0.07	0.08	12.08
1Cz5	0.02	0.03	0.81	0.40	0.47	82.71	0.04	0.04	0.04	0.75	0.74	0.75	0.78	70	74	84.7	75.9	80.3	1510.0	0.03	0.02	0.03	7.74
Brzeszcze 1	0.07	0.13	1.67	1.26	1.34	21.26	0.11	0.12	0.12	0.19	0.18	0.19	0.31	25	28	125.8	101.8	113.8	263.8	0.30	0.24	0.27	10.33
Brzeszcze 2	0.06	0.10	1.69	1.09	1.22	18.78	0.10	0.11	0.10	0.17	0.17	0.17	0.28	23	25	123.0	102.0	112.5	270.0	0.24	0.20	0.22	8.75
Brzeszcze 3	0.09	0.17	2.40	1.69	1.70	40.57	0.15	0.15	0.15	0.37	0.35	0.36	0.52	39	45	109.1	83.4	96.3	278.8	0.24	0.18	0.21	9.90
Brzeszcze 5	0.07	0.13	1.73	1.37	1.00	49.97	0.12	0.09	0.11	0.45	0.40	0.43	0.54	45	49	72.0	59.7	65.9	297.3	0.17	0.14	0.15	11.32
Brzeszcze 7	0.13	0.24	1.60	1.19	1.32	54.53	0.11	0.12	0.11	0.50	0.45	0.47	0.59	52	55	66.0	58.2	62.1	298.4	0.25	0.22	0.24	18.72
Brzeszcze 8	0.06	0.10	1.39	1.09	0.93	50.52	0.10	0.08	0.09	0.46	0.40	0.43	0.52	48	50	66.4	60.7	63.5	344.5	0.12	0.11	0.11	9.99
Brzeszcze 9	0.06	0.10	1.74	1.30	0.74	44.65	0.12	0.07	0.09	0.41	0.35	0.38	0.47	43	45	77.3	70.0	73.6	357.0	0.13	0.12	0.12	9.89

USCB, the ratio of B/N (expressed in ppm as B/(NH<sub>4</sub>)<sub>2</sub>O) was well constrained and increased from 0.01 to 0.1 in the course of illitization (Figure 10). The values for USCB bentonites were much larger due to both large B and small N contents.

## DISCUSSION AND CONCLUSIONS

(1) The present study was performed on raw rocks in order to study the entire budget of B and N, including their exchangeable forms, which could have been lost in the course of clay-fraction separation. The results document multi-fold increases of both elements in the authigenic 2:1 clay in the course of illitization. Such large increases cannot be attributed to an illitization reaction which would involve reduction of the mass of the clay by dissolution of the original smectite and precipitation of illite, concentrating both elements, originally adsorbed on smectite and then released during its dissolution. Such an interpretation can be excluded, based on sedimentary structures, perfectly conserved in their original geometry in the USCB bentonite bed (Środoń, 1974). Thus, the results indicate that the smectite illitization reaction over the range of 100 to <20%S is not so much the result of redistribution of existing B and N in the original smectite as it is a net extraction of both B and N from the pore waters. The contribution of B and N from parent smectite is rather small (Figure 7; extrapolations close to zero for pure smectite). This conclusion should be verified by selective extraction and measurements of the exchangeable forms of B and N.

(2) The case studied is different from regular sedimentary clays because the smectite in bentonitic horizons is not detrital but it crystallizes *in situ* during early diagenesis at the expense of volcanic glass. The conclusions drawn above refer only to this particular case. In shales dominated by detrital expandable clays, the proportion of exchangeable 'smectitic' B can be greater (Spivack *et al.*, 1987; Table 1 of Williams and Hervig, 2002, data for the Gulf Coast). Also, for ammonium, some studies indicate its quite elevated pure smectite contents, while others report decreases to zero at large expandabilities (Schroeder and McLain, 1998). Direct comparison is difficult, as all previous studies were performed on clay fractions and not on the untreated bulk rocks. A study performed by the same technique of interbedded shale and bentonite is needed.

(3) The present study demonstrates that bentonite acquires both B and N from outside of the bentonite bed. In one diagenetic cycle, bentonitic illite fixes up to 800–1000 ppm B and up to >1% (NH<sub>4</sub>)<sub>2</sub>O, *i.e.* >20% of fixed cation sites (Figure 9). These numbers result from assigning all measured B and N to the authigenic illite layers.

(4) Contrary to the opinions of several authors (*e.g.* Williams and Ferrell, 1991; Schroeder and McLain,

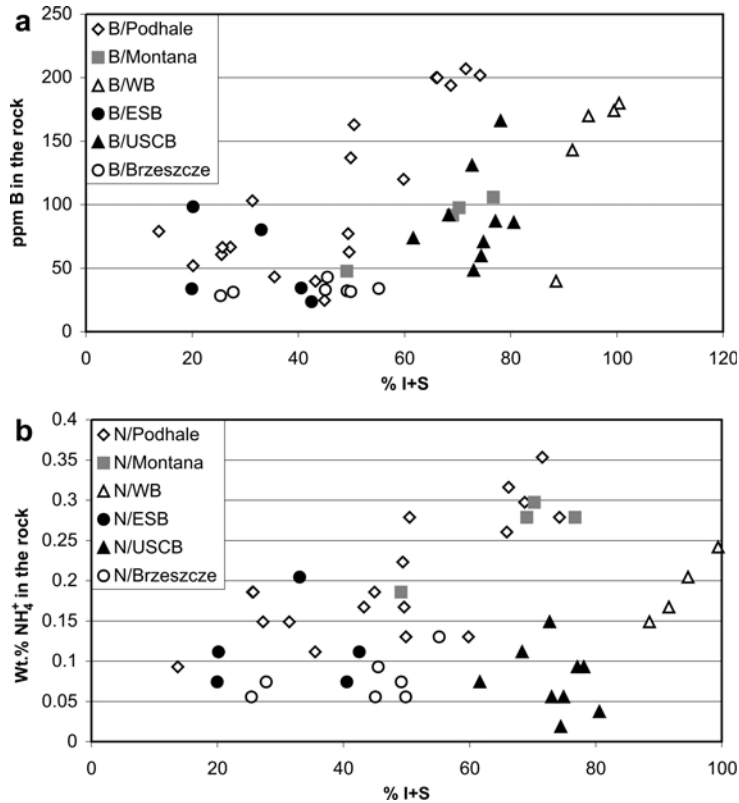


Figure 6. Boron (a) and ammonium (b) in the rock as functions of %I+S from XRD, plotted separately for different regions: WB – Welsh Borderlands, ESB – East Slovak Basin, USCBrzeczce – Upper Silesia Coal Basin (Brzeczce sample set plotted separately).

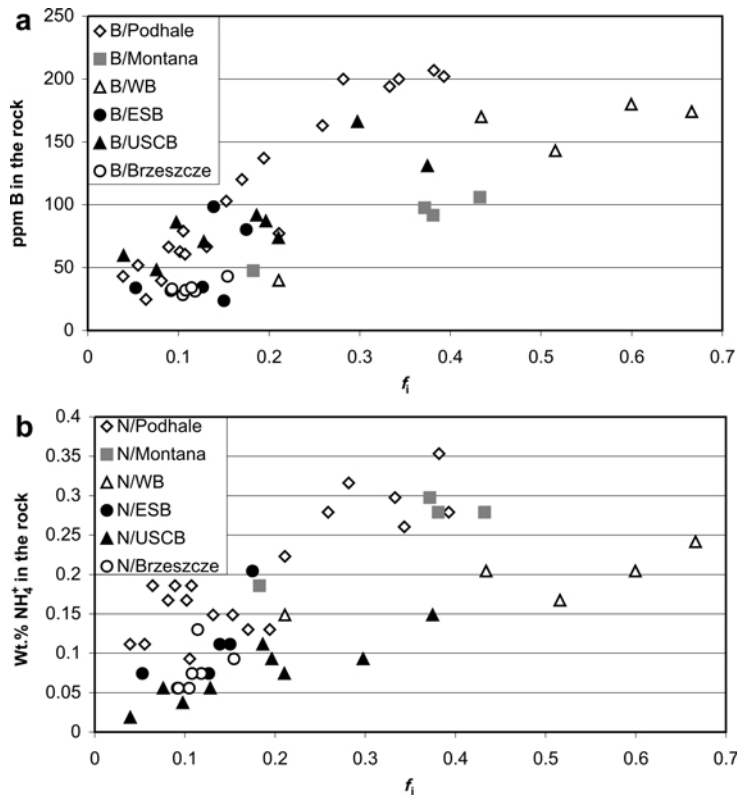


Figure 7. Boron (a) and ammonium (b) in the rock as functions of the fraction of illite, plotted separately for different regions.

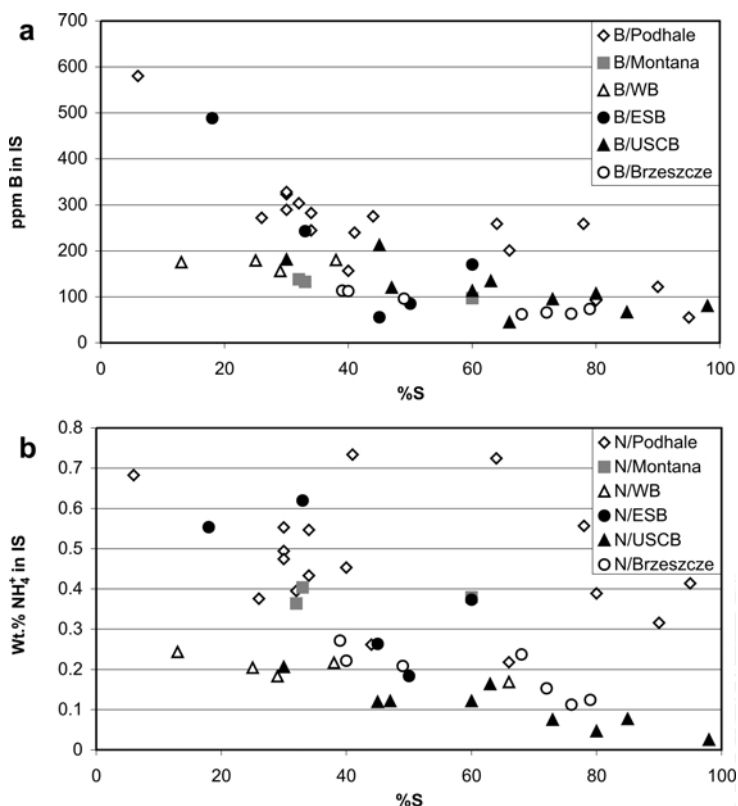


Figure 8. Boron (a) and ammonium (b) in illite-smectite as a function of the degree of diagenesis, expressed as percent smectite in illite-smectite (%S), plotted separately for different regions.

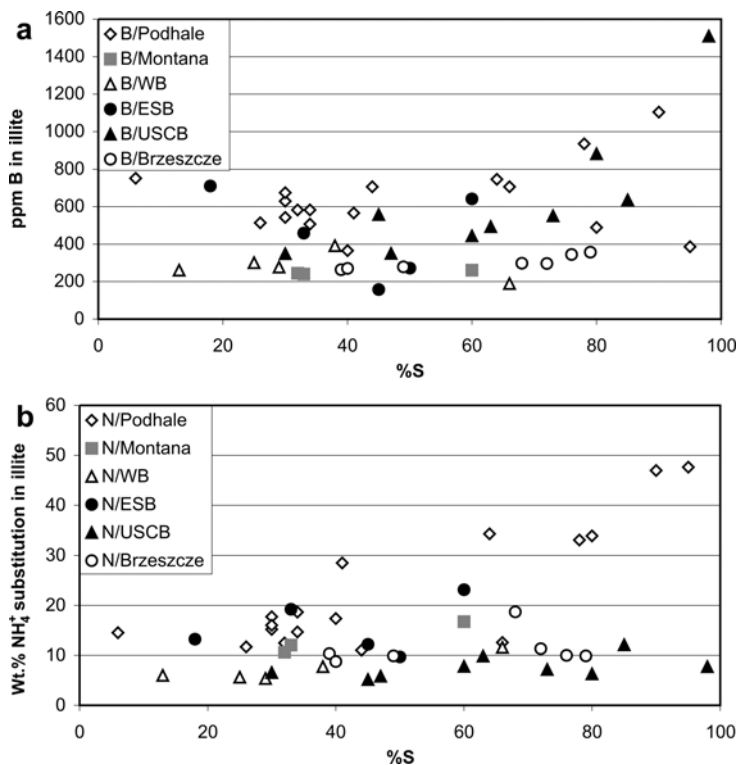


Figure 9. Boron (a) and ammonium (b) in illite as a function of the degree of diagenesis, expressed as percent smectite in illite-smectite (%S), plotted separately for different regions.

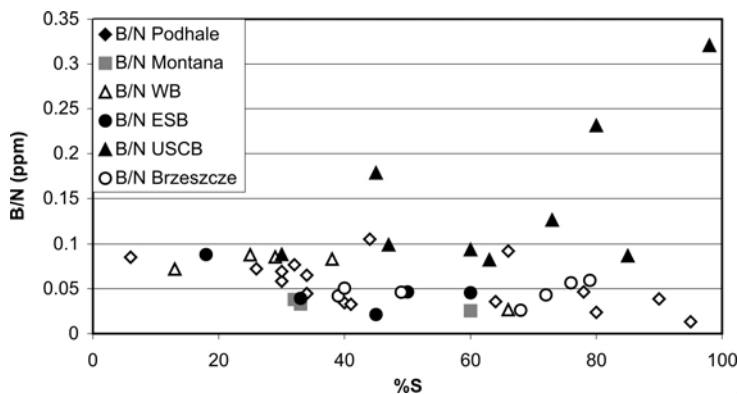


Figure 10. B/N ratio in illite (calculated in ppm) as a function of the degree of diagenesis, expressed as percent smectite in illite-smectite (%S), plotted separately for different regions.

1998; Lindgreen *et al.*, 2000), drawn from the studies of more complex systems, *i.e.* shales, this paper documents the illitic ammonium decrease in the course of diagenesis, including the oil-window temperature range. A similar tendency, though not as strong, was observed for B. These findings, based on interpreting all B and N as contained in illite, should be verified by studying the B and N contents of different classes of illite fundamental particles, which reflect subsequent stages of illite nucleation and growth (Clauer *et al.*, 1997; Środoń *et al.*, 2000, 2002).

(5) The remaining, intriguing question is whether these tendencies reflect a control by crystal-chemical properties of illite, by kinetics of illitization, or by pore-water composition. The first explanation seems to be favored by the fact that these tendencies were observed both in the sample sets representing bentonites from different depth in a basin (more illitic = higher temperature) and in zoned bentonite beds (more illitic = equal or lower temperature; see Clauer *et al.*, 1997). However, the N contents of illite are smallest in the USCB series, coming from a coal basin and rich in organic sources of this element, while greatest in Podhale bentonites, coming from a basin with small organic contents (TOC of shales = 0.1–3%: Kotarba, 2003; Marynowski *et al.*, 2006). Perhaps the thickness of the bentonite beds is also a factor; among the studied samples, the Podhale beds are the thinnest and the USCB bed is the thickest. Perhaps the kinetics of illite crystallization *vs.* the kinetics of B and  $\text{NH}_4^+$  supply controls the contents of these elements in the illite structure. In any case, during burial diagenesis, a bentonite layer was an open system with respect to these elements, but the scale of their migration remains unknown. This result supports earlier hypotheses concerning the origin of ammonium in illite, based on the studies of shales (Cooper and Abedin, 1981; Schroeder and McLain, 1998).

(6) Similarities in the diagenetic evolution of the B and N contents of illite, documented in the present study, argue in favor of the kerogen as the dominant common

source of both elements in sedimentary basins (see Williams *et al.*, 2001). Verifying the origin of B and deciphering the distances of migration of B and  $\text{NH}_4^+$  will require very detailed basin-scale studies, which may later help to interpret past hydrocarbon-forming processes from the record preserved in bentonites.

#### ACKNOWLEDGMENTS

Conversations with Dr Mariusz Paszkowski and Prof. A. Zuber inspired the author to undertake this study. Mrs. Dorota Bakowska is acknowledged for the chemical measurements, Dr Tadeusz Kawiak for collecting the XRD data, and Dr Leszek Chudzikiewicz for his help with editing the figures. Both the language and merit of the paper benefited from the reading by Lynda Williams.

#### REFERENCES

- Altaner, S.P., Hower, J., Whitney, G., and Aronson, J.L. (1984) Model for K-bentonite formation: Evidence from zoned K-bentonites in the Disturbed Belt, Montana. *Geology*, **12**, 412–425.
- Bardon, C., Bieber, M.T., Cuiec, L., Jacquin C., Courbot, A., Deneuille, G., Simon, J.M., Voirin, J.M., Espy, M., Nectoux, A., and Pellerin, A. (1983) Recommendations pour la détermination expérimentale de la capacité d'échange de cations des milieux argileux. *Revue de l'Institut Français du Pétrole*, **38**, 621–626.
- Basset, R.L. (1976) The geochemistry of boron in thermal waters. PhD thesis, Stanford University, California, USA.
- Berner, R.A. (2006) Geological nitrogen cycle and atmospheric  $\text{N}_2$  over Phanerozoic time. *Geology*, **34**, 413–415.
- Bobos, I. and Ghergari, L. (1999) Conversion of smectite to ammonium illite in the hydrothermal system of Harghita Bai, Romania: SEM and TEM investigations. *Geologia Carpathica*, **50**, 379–387.
- Clauer, N., Środoń, J., Franců J., and Šucha, V. (1997) K-Ar dating of illite fundamental particles separated from illite-smectite. *Clay Minerals*, **32**, 181–196.
- Collins, A.G. (1975) *Geochemistry of Oilfield Waters*. Elsevier, New York, 496 pp.
- Cooper, J.E. and Abedin, K.Z. (1981) The relationship between fixed ammonium-nitrogen and potassium in clays from a deep well on the Texas Gulf Coast. *Texas Journal of Science*, **33**, 103–111.
- Cooper, J.E. and Raabe, B.A. (1982) The effect of thermal gradient on the distribution of nitrogen in a shale. *Texas*

- Journal of Science*, **34**, 175–182.
- Daniels, E.J. and Altaner, S.P. (1990) Clay mineral authigenesis in coal and shale from the Anthracite region, Pennsylvania. *American Mineralogist*, **75**, 825–839.
- Ellis, D.V. and Singer, J.M. (2007) *Well Logging for Earth Scientists*. Springer, Berlin, 692 pp.
- Frederickson, A.F. and Reynolds, R.C., Jr. (1960) Geochemical method for determining paleosalinity. *Clays and Clay Minerals*, Proceedings of the Eighth National Conference, p. 202.
- Goldschmidt, V.M. and Peters, C. (1932) *Geochemie des Bors: I, II*. *Nachr. Ges. Wiss., Göttingen, Math-physik Kl*, 402–407, 528–545.
- Harder, H. (1970) Boron content of sediments as a tool in facies analysis. *Sedimentary Geology*, **4**, 153–175.
- Holloway, J.M. and Dahlgren, R. (1999) Geologic nitrogen in terrestrial biogeochemical cycling. *Geology*, **27**, 567–570.
- Jackson, M.L. (1975) *Soil Chemical Analysis – Advanced Course*. Published by the author, Madison, Wisconsin, USA.
- Keren, R. and Mezuman, V. (1981) Boron adsorption by clay minerals using a phenomenological equation. *Clays and Clay Minerals*, **29**, 198–204.
- Kotarba, M. (2003) Diagenetic history of illite-smectite in shales of the Western Carpathians (cross-section Krakow-Zakopane). PhD thesis, Institute of Geological Sciences PAN, Kraków (in Polish).
- Kozáč, J., Očenáš, D., and Derco, J. (1977) Amónna hydrosľuda vo Vihorlate. *Mineralia Slovaca*, **9**, 479–494 (in Slovak).
- Leeman, W.P. and Sisson, V.B. (1996) Geochemistry of boron and its implications for crustal and mantle processes. Pp. 645–707 in: *Boron Mineralogy, Petrology and Geochemistry* (E.S. Grew and L.M. Anovitz, editor). Reviews in Mineralogy, **33**, Mineralogical Society of America, Washington, D.C.
- Lindgreen, H. (1994) Ammonium fixation during illite-smectite diagenesis in Upper Jurassic shale, North Sea. *Clay Minerals*, **29**, 527–538.
- Lindgreen, H., Drits, V.A., Sakharov, B.A., Salyn, A.L., Wrang, P., and Dainyak, L.G. (2000) Illite-smectite structural changes during metamorphism in black Cambrian Alum shales from the Baltic area. *American Mineralogist*, **85**, 1223–1238.
- Marynowski, L., Gawęda, A., Poprawa, P., Żywiecki, M.M., Kępińska, B., and Merta, H. (2006) Origin of organic matter from tectonic zones in the Western Tatra Mountains Crystalline Basement, Poland: An example of bitumen–source rock correlation. *Marine and Petroleum Geology*, **23**, 261–279.
- Mingram, B., Hoth, P., Luders, V., and Harlov, D. (2005) The significance of fixed ammonium in Palaeozoic sediments for the generation of nitrogen-rich natural gases in the North German Basin. *International Journal of Earth Science*, **94**, 1010–1022.
- Mystkowski, K., Środoń, J., and McCarty, D.K. (2002) Application of evolutionary programming to automatic XRD quantitative analysis of clay-bearing rocks. *The Clay Minerals Society 39<sup>th</sup> Annual Meeting, Boulder, Colorado, Abstracts with Programs*.
- Newman, A.C.D. (1983) The specific surface of soils determined by water sorption. *Journal of Soil Science*, **34**, 23–32.
- Omotoso, O., McCarty, D.K., Hillier, S., and Kleeberg, R. (2006) Some successful approaches to quantitative mineral analysis as revealed by the 3<sup>rd</sup> Reynolds Cup contest. *Clays and Clay Minerals*, **54**, 748–760.
- Orsini, L. and Remy, J.-C. (1976) Utilisation du chlorure de cobaltihexammine pour la détermination simultanée de la capacité d'échange et des bases échangeables des sols. *Science du Sol*, **4**, 269–275.
- Palmer, M.R., Spivack, A.J., and Edmond, J.M. (1987) Temperature and pH controls over isotopic fractionation during adsorption of boron on marine clay. *Geochimica et Cosmochimica Acta*, **51**, 2319–2323.
- Perry, E.A. (1972) Diagenesis and the validity of the boron paleosalinity technique. *American Journal of Science*, **272**, 150–160.
- Reynolds, R.C., Jr. (1965) Geochemical behavior of boron during the metamorphism of carbonate rocks. *Geochimica et Cosmochimica Acta*, **29**, 1101–1114.
- Schroeder, P.A. and McLain, A.A. (1998) Illite-smectites and the influence of burial diagenesis on the geochemical cycling of nitrogen. *Clay Minerals*, **33**, 539–546.
- Spivack, A.J., Palmer, M.R., and Edmond, J.M. (1987) The sedimentary cycle of the boron isotopes. *Geochimica et Cosmochimica Acta*, **51**, 1939–1949.
- Šucha, V., Kraus, I., Gerthofferova, H., Petes, J. and Serekova, M. (1993) Smectite to illite conversion in bentonites and shales of the East Slovak Basin. *Clay Minerals*, **28**, 243–253.
- Šucha, V., Kraus, I., and Madejová, J. (1994) Amonum illite from anchimetamorphic shales associated with anthracite in the Zemplinicum of the Western Carpathians. *Clay Minerals*, **29**, 369–377.
- Środoń, J. (1974) An interpretation of climbing-ripple cross-lamination. *Annales Societatis Geologorum Poloniae*, **44**, 449–473.
- Środoń, J. (1976) Mixed-layer smectite/illites in the bentonites and tonsteins of the Upper Silesian Coal Basin. *Prace Mineralogiczne*, **49**, 7–84.
- Środoń, J. (1980) Precise identification of illite/smectite interstratifications by X-ray powder diffraction. *Clays and Clay Minerals*, **28**, 401–411.
- Środoń, J. (1984) X-ray powder diffraction identification of illitic materials. *Clays and Clay Minerals*, **32**, 337–349.
- Środoń, J. (2009) Quantification of illite and smectite and their layer charges in sandstones and shales from shallow burial. *Clay Minerals*, **44**, 417–430.
- Środoń, J. and McCarty, D.K. (2008) Surface area and layer charge of smectite from CEC and EGME/H<sub>2</sub>O retention measurements. *Clays and Clay Minerals*, **56**, 142–161.
- Środoń, J., Morgan, D., Eslinger, E.V., Eberl, D.D., and Karlinger, M.R. (1986) Chemistry of illite/smectite and end-member illite. *Clays and Clay Minerals*, **34**, 368–378.
- Środoń, J., Eberl, D.D., and Drits, V.A. (2000) Evolution of fundamental particle size during illitization of smectite and implications for reaction mechanism. *Clays and Clay Minerals*, **48**, 446–458.
- Środoń, J., Drits, V.A., McCarty, D.K., Hsieh, J.C.C., and Eberl, D.D. (2001) Quantitative XRD analysis of clay-rich rocks from random preparations. *Clays and Clay Minerals*, **49**, 514–528.
- Środoń, J., Clauer, N., and Eberl, D.D. (2002) Interpretation of K-Ar dates of illitic clays from sedimentary rocks aided by modelling. *American Mineralogist*, **87**, 1528–1535.
- Środoń, J., Kotarba, M., Biro, A., Such, P., Clauer, N., and Wójtowicz, A. (2006a) Diagenetic history of the Podhale-Orava basin and the underlying Tatra sedimentary structural units (Western Carpathians): evidence from XRD and K-Ar of illite-smectite. *Clay Minerals*, **41**, 747–770.
- Środoń, J., Clauer, N., Banaś, M., and Wójtowicz, A. (2006b) K-Ar evidence for a Mesozoic thermal event superimposed on burial diagenesis of the Upper Silesia Coal Basin. *Clay Minerals*, **41**, 671–692.
- Środoń, J., Clauer, N., Huff, W., Dudek, T., and Banaś, M. (2009a) K-Ar dating of Ordovician bentonites from the Baltic Basin and the Baltic Shield: implications for the role of temperature and time in the illitization of smectite. *Clay*

- Minerals*, **44**, 361–387.
- Środoń, J., Zeelmaekers, E., and Derkowski, A. (2009b) The charge of component layers of illite-smectite in bentonites and the nature of end-member illite. *Clays and Clay Minerals*, **57**, 650–672.
- Tiller, K.G. and Smith, L.H. (1990) Limitations of EGME retention to estimate the surface area of soils. *Australian Journal of Soil Research*, **28**, 1–26.
- Williams, L.B. and Ferrell, R.E., Jr. (1991) Ammonium substitution in illite during maturation of organic matter. *Clays and Clay Minerals*, **39**, 400–408.
- Williams, L.B., Wilcoxon, B.R., Ferrell, R.E. Jr., and Sassen, R. (1992) Diagenesis of ammonium during hydrocarbon maturation and migration, Wilcox Group, Louisiana, USA. *Applied Geochemistry*, **7**, 123–134.
- Williams, L.B., Ferrell, R.E. Jr., Hutcheon, I., Bakel, A.J. Walsh, M.M., and Krouse, H.R. (1995) Nitrogen isotope geochemistry of organic matter and minerals during diagenesis and hydrocarbon migration. *Geochimica et Cosmochimica Acta*, **59**, 765–779.
- Williams, L.B., Havig, R.L., Wieser, M.E., and Hutcheon, I. (2001) The influence of organic matter on the boron isotope geochemistry of the Gulf Coast Sedimentary Basin, USA. *Chemical Geology*, **174**, 445–461.
- Williams, L.B. and Havig, R.L. (2002) Exploring intracrystalline B-isotope variations in mixed-layer illite-smectite. *American Mineralogist*, **87**, 1564–1570.
- You, C.F., Spivack, A.J., Gieskes, J.M. Rosenbauer, R., and Bischoff, J.L. (1995) Experimental study of boron geochemistry: Implications for fluid processes in subduction zones. *Geochimica et Cosmochimica Acta*, **59**, 2435–2442.
- Zorski, T., Ossowski, A., Środoń, J., and Kawiak, T. (2011) Evaluation of mineral composition and petrophysical parameters from well logging data: the Carpathian Foredeep case study. *Clay Minerals* (in press).
- Zuber, A. and Chowanec, J. (2009) Diagenetic and other highly mineralized waters in the Polish Carpathians. *Applied Geochemistry*, **24**, 1889–1900.

(Received 1 July 2010; revised 27 October 2010; Ms. 454; A.E. L.B. Williams)